SPECIAL TOPIC — Physical research in liquid crystal

Determining the imaging plane of a retinal capillary layer in adaptive optical imaging*

Le-Bao Yang(杨乐宝)[1,2], Li-Fa Hu(胡立发)[1], Da-Yu Li(李大禹)[1], Zhao-Liang Cao(曹召良)[1], Quan-Quan Mu(穆全全)[1], Ji Ma(马骥)[1,3], and Li Xuan(宣丽)[1,†]

[1] *State Key Laboratory of Applied Optics, Changchun Institute of Optics, Fine Mechanics and Physics, Chinese Academy of Sciences, Changchun* 130033, *China*

[2] *University of Chinese Academy of Sciences, Beijing* 100049, *China*

[3] *Liquid Crystal Institute, Kent State University, Kent* 44242, *USA*

(Received 19 May 2016; published online 20 July 2016)

Even in the early stage, endocrine metabolism disease may lead to micro aneurysms in retinal capillaries whose diameters are less than 10 μm. However, the fundus cameras used in clinic diagnosis can only obtain images of vessels larger than 20 μm in diameter. The human retina is a thin and multiple layer tissue, and the layer of capillaries less than 10 μm in diameter only exists in the inner nuclear layer. The layer thickness of capillaries less than 10 μm in diameter is about 40 μm and the distance range to rod&cone cell surface is tens of micrometers, which varies from person to person. Therefore, determining reasonable capillary layer (CL) position in different human eyes is very difficult. In this paper, we propose a method to determine the position of retinal CL based on the rod&cone cell layer. The public positions of CL are recognized with 15 subjects from 40 to 59 years old, and the imaging planes of CL are calculated by the effective focal length of the human eye. High resolution retinal capillary imaging results obtained from 17 subjects with a liquid crystal adaptive optics system (LCAOS) validate our method. All of the subjects' CLs have public positions from 127 μm to 147 μm from the rod&cone cell layer, which is influenced by the depth of focus.

Keywords: liquid crystal device, adaptive optics, capillary layer position, retinal imaging

PACS: 42.70.Df, 42.68.Wt, 42.66.Lc **DOI:** 10.1088/1674-1056/25/9/094219

1. Introduction

Imaging for retinal capillaries is an important technique for diagnosing endocrine metabolism disease, such as diabetes[1–4] and cardiovascular disease.[5,6] The retinas of subjects with non-proliferative diabetic retinopathy (NPDR) have numerous vessel abnormalities, like capillary doubling loop or loops and micro aneurysms. The diameter of the injury capillaries is less than 10 μm in the early stage of endocrine metabolism disease.

The retina consists of ten layers of translucent tissues. The capillary layer (CL) only exists in one layer with the thickness about 30 μm,[7–9] and from person to person the varied range of CL position is about 20 μm. The fundus cameras and fundus fluorescein angiography (FFA) that have recently been used in clinic diagnosis can only obtain images of blood vessels more than 20 μm in diameter. The blood vessels are easy to obtain without determining the imaging plane, while it is difficult to capture CL, which is limited by the eye aberration and the imaging plane determining of the CL.

With the help of an adaptive optics system (AOS), some groups have obtained images of capillaries that are less than 10 μm in diameter.[10–14] However, AOS cannot always capture CL for different persons. The position determining problem is the bottleneck for retinal imaging in AOS applied in clinical diagnosis. This problem is mainly caused by the following factors: first, the imaging of CL should be quickly obtained, within tens of milliseconds; second, the depth of field is about 30 μm, which is approximate to the thickness of CL, while the distance range of CL position is tens micrometer from person to person, thus making it difficult to capture the CL; third, given that the effective focal length is different in persons, it cannot determine the imaging plane of CL with the CL position in the retina.

There is no reference discussing how to determine the capillary imaging position. Usually, researchers determine the capillary imaging position by searching for a retinal capillary image by moving the detector backward or forward[15,16] or using optical coherence tomography (OCT)[17] to achieve retinal tomography images. But these cannot capture the CL for different human eyes.

In order to solve the capillary imaging plane determining problem and obtain high resolution images of the capillaries in different human eye, a reasonable position of the capillary imaging is proposed. In this paper, a method is proposed to calculate the reasonable imaging plane position of retinal capillary images based on the rod&cone cell surface. The theory of a capillary imaging plane is described in Section 2. The experimental setup on liquid crystal adaptive optics system

*Project supported by the National Natural Science Foundation of China (Grant Nos. 11174274, 11174279, 61205021, 11204299, 61475152, and 61405194).

†Corresponding author. E-mail: xuanli1957@sina.com

© 2016 Chinese Physical Society and IOP Publishing Ltd

(LCAOS) is given in Section 3, and the experimental results are discussed in Section 4. Finally, the conclusion is given in Section 5.

2. Theory

The images of rod&cone cells are easily captured with AOS[18,19] because that the imaging position of the rod&cone cell is exactly in the focal plane of the last lens in AOS. Figure 1 shows the conjugate relationship between the CL imaging position and the CL position in the retina. To observe the capillary images, it is necessary to move the retinal camera to a position L away from the focal plane, as shown in Fig. 1. L could be calculated as

$$L = \alpha L_{\mathrm{cc}}, \tag{1}$$

where L_{cc} is the distance between the rod&cone cell and the CL, and α is the longitudinal magnification of the LCAOS. Since the refractive index of biological tissue in retina is complex, the effective focal length (EFL) is used to calculate α, given by

$$\alpha = (f_1 f_3/f_2)^2/\mathrm{EFL}_{\mathrm{eye}}^2 = K/\mathrm{EFL}_{\mathrm{eye}}^2, \tag{2}$$

where f_1, f_2, and f_3 are the focal length of the lens L1, L2, and L3, respectively, $K = (f_1 f_3/f_2)^2$ is the structure coefficient of LCAOS, and $\mathrm{EFL}_{\mathrm{eye}}$ is the effective focal length of the human eye.

Substituting Eq. (2) into Eq. (1), we get

$$L = K L_{\mathrm{cc}}/\mathrm{EFL}_{\mathrm{eye}}^2. \tag{3}$$

It is obvious that L depends on the values of L_{cc} and $\mathrm{EFL}_{\mathrm{eye}}$, which are calculated in the following sections.

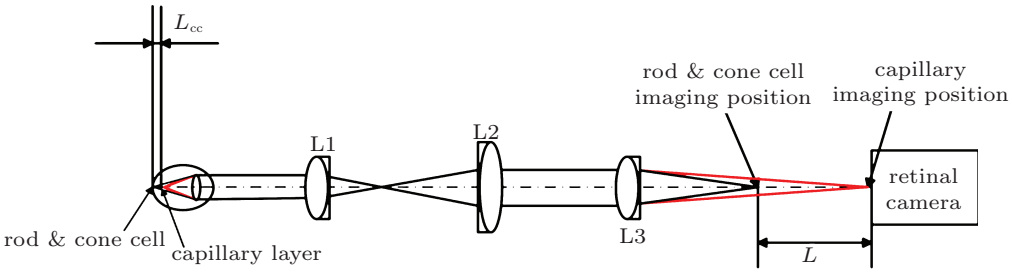


Fig. 1. (color online) A schematic of the conjugate relation between the CL and the position of the retinal camera. Here L_{cc} is the distance between the rod&cone cell and CL, L is the distance between the rod&cone cell imaging position and the retinal capillary imaging position, and L1–L3 denote the lenses.

3. The distance between the rod&cone cell and capillary layer L_{cc}

The retina mainly includes three kinds of cells: the ganglion cell, the bipolar cell, and the rod & cone cell, as shown in Fig. 2. The retina is mainly divided into 10 layers, and the big blood vessels are distributed among the ganglion cell layer (GCL) and the inner plexiform layer (IPL), while the inner nuclear layer (INL) is supposed to be CL because the capillaries less than 10 μm in diameter are to be found in INL.

The thickness mapping of retina from optical coherence tomography (SD-OCT)[9] is given in Table 1 and the subjects are aged from 40 to 59.

Table 1. Thickness mapping of retinal layers.

	ONL+IS/μm	OPL/μm	INL/μm
superior	80±12	37±6	37±3
inferior	79±8	40±6	38±2
temporal	81±7	37±5	36±2
nasal	81±8	41±6	39±3

The distance between the CL and rod&cone cell varies in different eyes. For convenience of observation, a public distance will be effective for most people during retinal capillary observation. The public distance L_{cc} and its range ΔL_{cc} are calculated as

$$L_{\mathrm{cc}} = (L_{\mathrm{cc\text{-}u}} - \mathrm{Std}_{\mathrm{cc\text{-}u}} + L_{\mathrm{cc\text{-}b}} + \mathrm{Std}_{\mathrm{cc\text{-}b}})/2, \tag{4}$$

$$\Delta L_{\mathrm{cc}} = (L_{\mathrm{cc\text{-}u}} - \mathrm{Std}_{\mathrm{cc\text{-}u}} - L_{\mathrm{cc\text{-}b}} - \mathrm{Std}_{\mathrm{cc\text{-}b}})/2, \tag{5}$$

where $L_{\mathrm{cc\text{-}b}}$ and $\mathrm{Std}_{\mathrm{cc\text{-}b}}$ represent the distance and the standard deviation between the bottom of the INL and the rod&cone cell, and $L_{\mathrm{cc\text{-}u}}$ and $\mathrm{Std}_{\mathrm{cc\text{-}u}}$ represent the distance and the standard deviation between the up of the INL and the rod&cone cell.

As shown in Table 2, the public positions L_{cc} and its variation ΔL_{cc} is 137.6 ± 8.1 μm. Another study[8] reported that the experimental result is 128.9 ± 7.6 μm, which is about 8.7 μm thinner than the result in Table 2. As the results of these two studies are similar, the public position L_{cc} in this article is chosen as 137.6 μm.

Table 2. Distance and the corresponding variation between the cell and INL

	$L_{\mathrm{cc\text{-}b}}$/ μm	$L_{\mathrm{cc\text{-}u}}$ / μm	L_{cc}/μm
superior	117 ±13.42	154±13.75	135.33 ±4.92
inferior	119 ±10.00	157 ±10.20	137.90 ±8.90
temporal	118 ±8.60	154 ±8.83	135.89 ±9.28
nasal	122 ±10.00	161 ±10.44	141.28 ±9.28
mean			137.60± 8.10

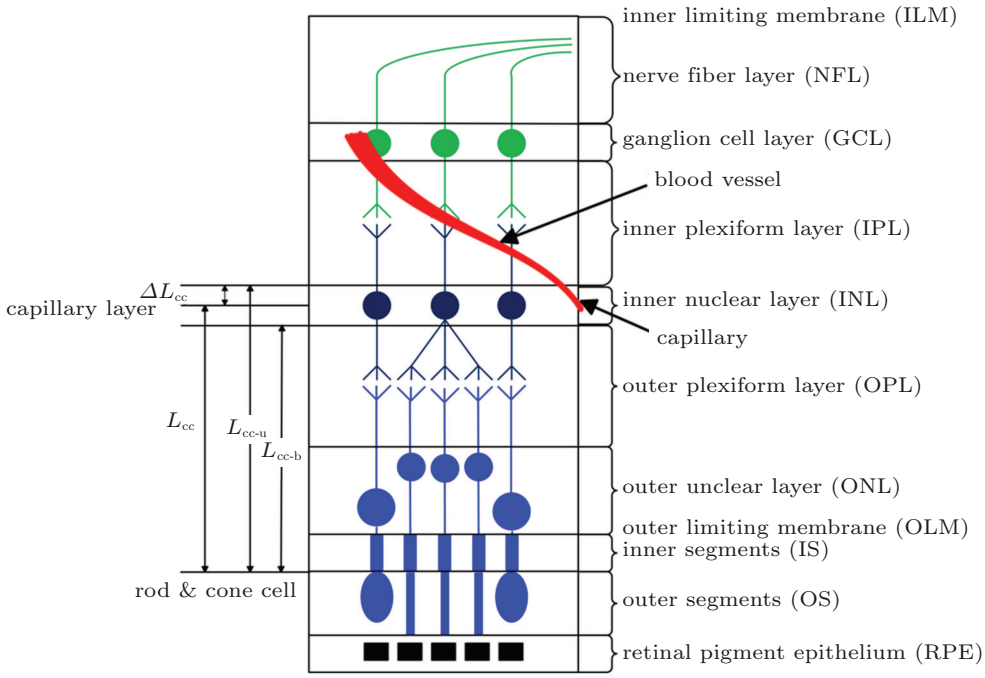


Fig. 2. (color online) A schematic diagram of the retina organization. The green cells represent the ganglion cells, the black cells represent bipolar cells, and the blue cells represent rods (center 3 cells) and cones (edge 2 cells). L_{cc} and ΔL_{cc} are the distance and its variation between CL and rod&cone cell. $L_{cc\text{-}u}$ is the maximum of L_{cc} and $L_{cc\text{-}b}$ is the minimum of L_{cc}.

4. The effective focal length of human eye EFL_{eye}

The imaging plane of CL also depends on the effective focal length of the human eye, EFL_{eye}, which can be calculated by measuring the length of axis oculi $L_{axisoculi}$ according to

$$EFL_{eye} = ML_{axisoculi} + C, \tag{6}$$

where M and C are the unknown parameters between the effective focal length EFL_{eye} and the axis length $L_{axisoculi}$.

LCAOS is similar to a dynamic trial lens to compensate the eye aberration in real time as shown in Fig. 3. A Gullstrand–Le Grand eye model and a reduced eye model[20,21] are used to calculate the EFL_{eye}. As shown in Fig. 3, an object with height H in the focal plane of lens L1 generates an image with height of h in eye model. The effective focal length of eye EFL_{eye} is calculated by

$$EFL_{eye} = Hf_1/h. \tag{7}$$

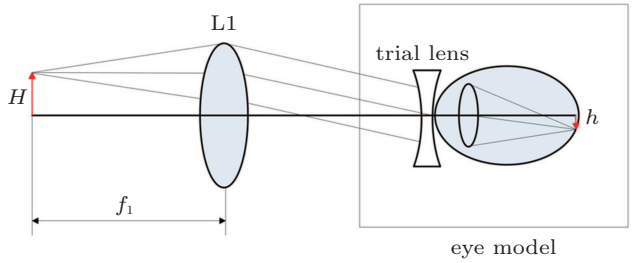


Fig. 3. (color online) Optical layout of the effective focal length of eye model testing.

Changing the diopter of trial lens from –10D to 10D, the simulated results with Zemax software of EFL_{eye} and $L_{axisoculi}$ are shown in Fig. 4 according to two eye models. The relationship between EFL_{eye} and $L_{axisoculi}$ is fitted by

$$EFL_{eye} = 0.7136 * L_{axisoculi} + 0.1483, \tag{8}$$

and the largest relative error of EFL_{eye} is ±4.4%.

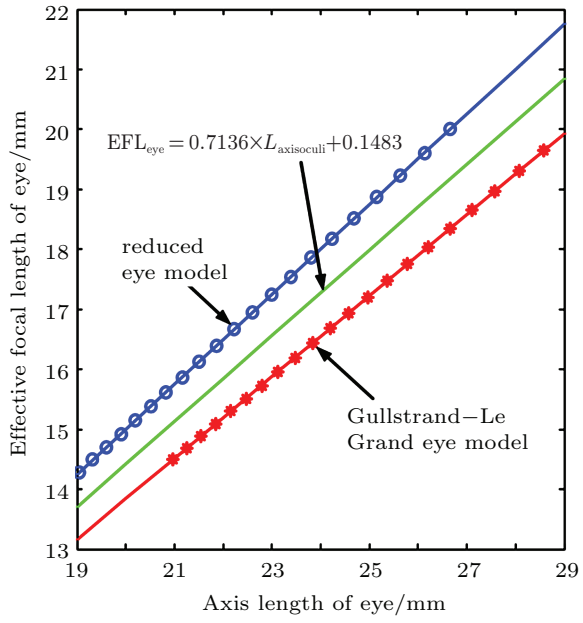


Fig. 4. (color online) The relationship between EFL_{eye} and $L_{axisoculi}$.

5. Experimental setup with LCAOS

In order to verify the calculation and method of imaging plane of CL, an open-loop LCAOS experiment is performed for capillary imaging detection. The case study is implemented with the LCAOS shown in Fig. 4 and 17 subjects. A Shack–Hartman wavefront sensor (SH-WFS) is used as wavefront detection for the eye, and a nematic liquid crystal spatial light modulator (LC-SLM)[22–24] is used in LCAOS for wavefront correction, which has 256×256 pixels and 1.8 ms response time at 45°C. The parameters of the SH-WFS and the LC-SLM are listed in Table 3.

Table 3. The parameters of the SH-WFS and the LC-SLM.

SH-WFS		LC-SLM	
Aperture	3×3 mm	Array size	6.14×6.14 mm
Subaperture diameter	150 μm	Active pixels	256×256
Lenslet focal length	3.2 mm	Response time	1.8 ms
Working wavelength	600–900 nm	Wavelength Range	760–865 nm
Measurement accuracy in relative mode (RMS)	1/100λ	Reflected wavefront distortion (RMS)	λ/10

The LCAOS mainly contains four subsystems, as shown in Fig. 5: (i) Illumination subsystem. This includes laser 1 (785 nm, CNI Inc., China) for wavefront detection and laser 2 (808 nm, CNI Inc., China) for retinal imaging. The illuminated area is 50 μm for wavefront detection and 350 μm for retinal imaging. Their powers incident on human eye are 50 μW and 300 μW, which are less than 1/50 maximum permissible exposure (MPE) recommended by ANSI.[25] Two rotating diffusers are used to reduce the influence of the speckle noise[26] before they are focused into fibers. The annular aperture (Aa) is used conjugated to the human eye pupil. (ii) Vision target subsystem. A green light emitting diode (LED, 530 nm) is used as the target source. Obviously, its wavelength is different from that of illumination subsystem. To compensate its axial chromatic[27] dispersion aberration between wavelength due to 1D difference between 530 nm and 785 nm, as the illumination source is at 0D position, the target source is at 1D position. (iii) Pupil monitoring subsystem. A pupil infrared light source (PIS) is used to illuminate the human eye. A camera is used to monitor the eye pupil which helps to align the eye in optical path precisely. (iv) Wavefront correction and imaging subsystem. LC-SLM is the main component of the wavefront correction system. High resolution retinal images are obtained after the aberration detection and compensation. In order to move CL imaging position, the retinal camera is installed on a movable stage driven by a servo motor.

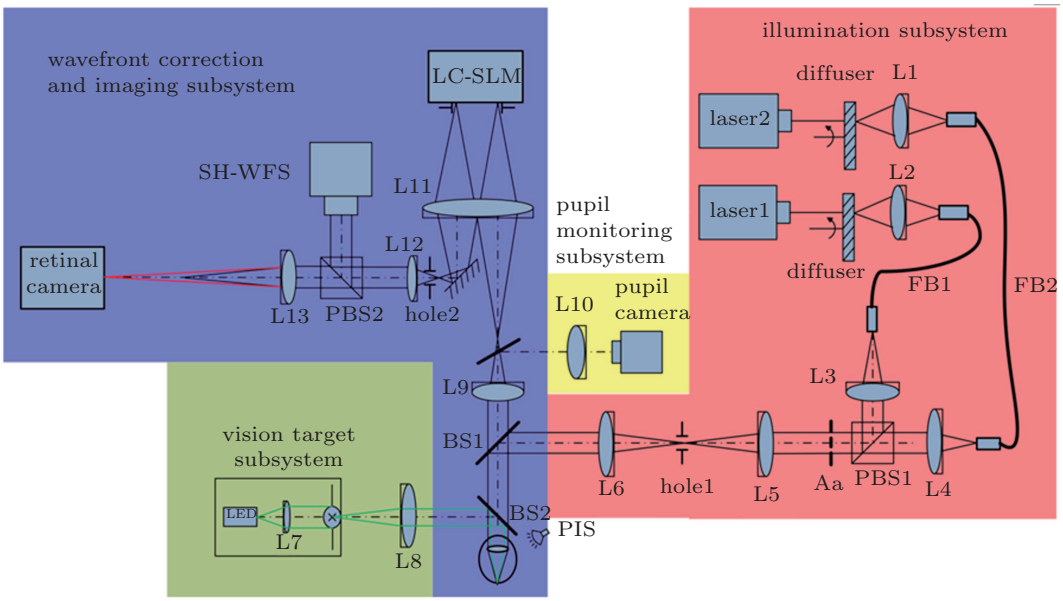


Fig. 5. (color online) Experiment layout of the open-loop LCAOS for capillary imaging. Here BS is the beam splitter, PBS is the polarizing beam splitter, and FB1 and FB2 are the optical fibers. Light red area represents the illumination subsystem, light green area represents the vision target subsystem, light yellow area represents the pupil monitoring subsystem, and light blue area represents the wavefront correction and imaging subsystem.

The sequential chart of AOS is shown in Fig. 6. Laser 1 and the charge coupled device (CCD) of the SH-WFS work on external trigger mode; that is, after triggered simultaneously by the external signal, laser 1 is on and CCD of SH-WFS starts exposure (3 ms) during the high level of the trigger signal. Then laser 1 is off, and light spots are read out within 2 ms processed by the industrial personal computer (IPC). The gray map is generated about 0.7 ms with IPC, and the gray map is loaded on LC-SLM with response time 1.8 ms. Next, the second trigger occurs so that laser 2 is on and the retinal camera simultaneously starts exposure for 8 ms. The next correction loop simply repeats the above steps. The cycle time is about

15.5 ms and the frequency of the LCAOS is 64.5 Hz.

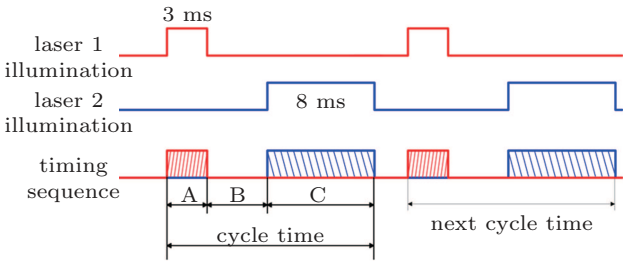


Fig. 6. (color online) The sequential chart of the open-loop AOS. Laser 1 and 2 are on once triggered by high level signal. A: exposure of SH-WFS'S CCD with 3 ms, B: data process time 4.5 ms, C: exposure of retinal camera with 8 ms.

6. Experimental results and discussion

The axis length of the eyes was tested with B-SCAN-CINESCAN from Quantel Medical, France, and the resolution is 40 μm which can be ignored. As shown in Table 4, 17 subjects were tested, whose ages are from 26 to 42 and the myopias are from –8D to 0D. The axis lengths are ranged from 23.54 mm to 27.77 mm.

Table 4. Parameters of the subjects

Subject	Eye case	Age	Myopia	Axis oculi/mm
GQL	Left	26	–1.5D	24.72
GQR	Right	26	–0.5D	24.58
MHR	Right	26	–5D	26.25
CCL	Left	27	–7D	27.08
GYR	Right	26	–6.5D	27.85
LCR	Right	26	–2D	23.54
ZYR	Right	27	0D	24.00
LYR	Right	27	–3D	25.00
SFR	Right	26	–3D	24.35
DYL	Left	36	–2.5D	25.40
DYR	Right	36	–2.5D	25.65
CLL	Left	33	–3D	24.20
CLR	Right	33	–4D	24.95
LFL	Left	42	–7D	27.30
LFR	Right	42	–7D	27.77
YKL	Left	27	–8D	27.22
YKR	Right	27	–8D	27.44

As shown in Fig. 7, the imaging results of six subjects' capillaries with the capillary position at 137 μm away from rod&cone cell are given. The results indicate that the sharpness images can be obtained by our method. The diameter of capillary on the distance 137 μm away from rod&cone cell is less than 10 μm.

To validate the expectations, a series of images with positions of CL in a range from 107 μm to 177 μm away from rod&cone cell are given. As shown in Fig. 8, two subjects' capillary images with the positions 107 μm to 177 μm away from rod&cone cell are given. The clear capillary images of subject 1 are positioned from 117 μm to 167 μm from rod&cone cell, while the clear capillary images of subject 2 are positioned from 117 μm to 147 μm from rod&cone cell.

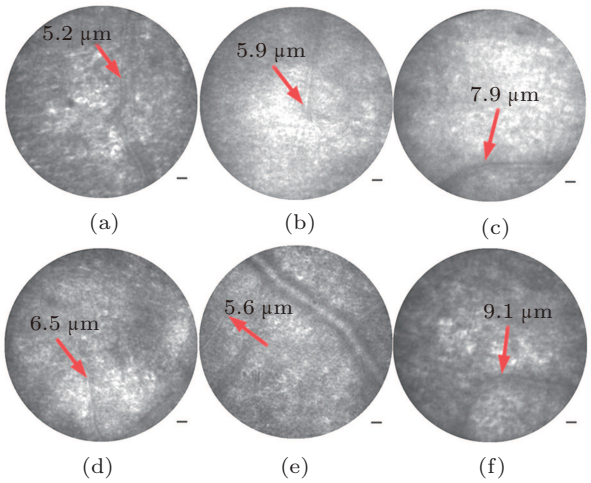


Fig. 7. (color online) Capillary images for six subjects. The capillary images are imaging at 137 μm away from rod&cone cell. Scale bar indicates 20 μm.

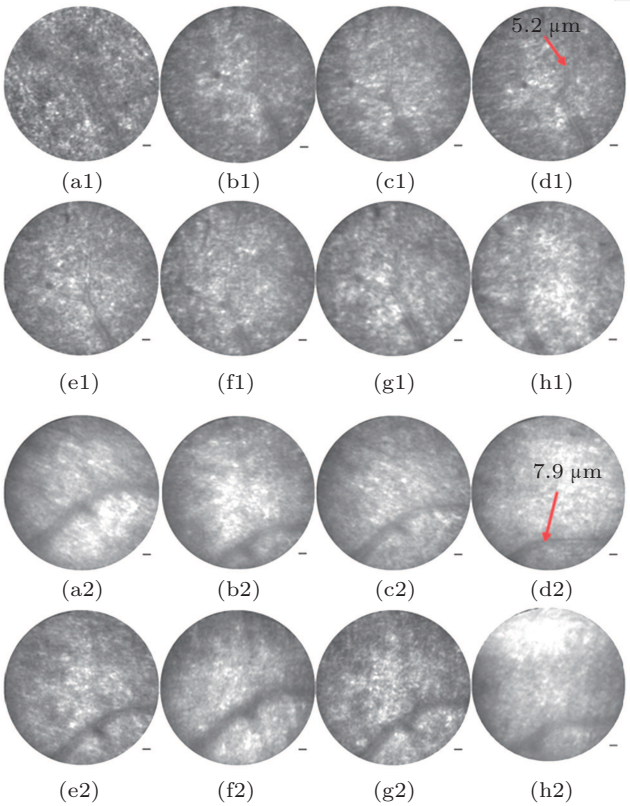


Fig. 8. (color online) Capillary images for 2 subjects with different imaging positions. (a)–(h) The capillary images imaging at 107 μm to 177 μm away from rod&cone cell. The clear capillary images of subject 1 are the imaging from 117 μm to 167 μm, and the subject 2 from 117 μm to 147 μm. Scale bar indicates 20 μm.

As EFL_{eye} is calculated by the axis length of the eye, the moving distance of retinal camera L and the position of capillary L_{eye} have a certain error. By calculating the differential of

Eq. (3), the relationship between the relative error of positions in the retina L_{eye} and the relative error of EFL_{eye} is given by

$$\delta L_{\text{eye}}/L_{\text{eye}} = 2\delta\text{EFL}_{\text{eye}}/\text{EFL}_{\text{eye}}. \tag{9}$$

The relative error of the CL positions is twice as large as the relative error of EFL_{eye}. Because the relative error of EFL_{eye} is $\pm 4.4\%$, the relative error of the L_{eye} is $\pm$ 8.8%.

In Fig. 9, a series of measured results of the CL positions are given for different subjects. The retinal capillaries could be seen clear at the positions, and the standard deviations are calculated based on the error of L_{eye}. It shows that public positions of the CL ranged from 127 μm to 147 μm away from rod&cone cell.

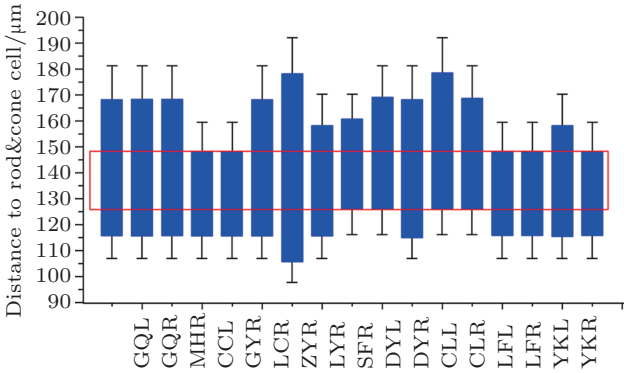


Fig. 9. (color online) The positions of the retinal capillaries in the focal plane for subjects. The red rectangle represents the public positions in different human eyes.

The sharpness of the capillary images is influenced by the depth of field[28] and depth of focus.[29] Considering the human eye as an optical system, the depth of field of the eye leads to the clear capillary images in the focus range. The depth of field in human eye can be calculated as

$$\Delta L = \frac{2Dp^2\varepsilon}{D^2 - p^2\varepsilon^2}, \tag{10}$$

where D is the diameter of entrance pupil, p is the distance between the entrance pupil and imaging plane, and ε is the eye limiting angle of resolution. When calculating the depth of field, p is 18 mm, ε is $1'$ and D is 6 mm for pupil. The depth of field is then about 31 μm.

The depth of focus is the amount of defocus that introduces a $\pm\lambda/4$ wavefront error, and the depth of focus can be calculated as

$$\Delta f = 4\lambda F^2, \tag{11}$$

where $\lambda = 0.808$ μm, that is the wavelength of illumination, and $F = 54.7$, that is the F number of the image space. Thus, the depth of focus Δf is 9.67 mm, which corresponds to 28.6 μm in the retina.

The depth of field is 31 μm, which means that the imaging of the CL position is about 31 μm when the imaging position is fixed. Because the public thickness of CL is about 20 μm, the public CL consists in the depth of field when the imaging plane is conjugated to 137 μm away from rod&cone cell.

With the results of experiment in 17 human eyes, the sharpness of capillary images can be shown to be acceptable on the position which is conjugated to 137 μm away from rod&cone cell. In addition, the public positions of CL are 127 μm to 147 μm away from rod&cone cell, which is similar to the depth of focus.

7. Conclusion

The public CL positions are recognized as 127 μm to 147 μm to rod&cone cell for subjects from 26 to 59 years old. The relationship between EFL_{eye} and the axis length of eye with two different eye models is applied to calculate the effective focal length of human eyes. With the positions of CL and the effective focal length, it is easy to capture the CL with LCAOS. Six subjects' capillary images are obtained with the CL position at 137 μm to rod&cone cell, and the diameter of capillary is less than 10 μm. A series of experiments with 17 subjects on LCAOS are used to validate our expectations. With the influence of depth of field, the imaging plane can be fixed on the position which is conjugated to 137 μm from rod&cone cell. The imaging positions of the capillaries are 124 μm to 147 μm, which is influenced by the depth of focus.

With our method, the problem of determining the position of the capillaries can be solved. This method can be transplanted into other AOS , such as scanning laser ophthalmoscope or OCT with AOS. We hope that this method will boost the development of clinical application of retinal capillary diagnosis in the future.

References

[1] Browning D J, Altaweel M M, Bressler N M, Bressler S B and Scott I U 2008 *Am. J. Ophthalmol.* **146** 649
[2] Tam J, Dhamdhere K P, Tiruveedhula P, Manzanera S, Barez S, Bearse M A, Adams A J and Roorda A 2011 *Invest. Ophthalmol. Vis. Sci.* **52** 9257
[3] Deak G G and Schmidt-Erfurth U 2013 *Curr. Diabetes. Rep.* **13** 469
[4] Burns S A, Elsner A E, Chui T Y, VanNasdale D A, Clark C A, Gast T J, Malinovsky V E and Phan A D T 2014 *Biomed. Opt. Express* **5** 961
[5] Zhu P, Huang F, Lin F, Li Q, Yuan Y, Gao Z and Chen F 2014 *PLoS One* **9** e106551
[6] Wang J J, Liew G, Klein R, Rochtchina E, Knudtson M D, Klein B E, Wong T Y, Burlutsky G and Mitchell P 2007 *Eur. Heart J.* **28** 1984
[7] Bagci A M, Shahidi M, Ansari R, Blair M, Blair N P and Zelkha R 2008 *Am. J. Ophthalmol.* **146** 679
[8] Tan O, Li G, Lu A T H, Varma R and Huang D 2008 *Ophthalmology* **115** 949
[9] Loduca A L, Zhang C, Zelkha R and Shahidi M 2010 *Am. J. Ophthalmol.* **150** 849
[10] Ling N, Zhang Y, Rao X, Wang C, Hu Y and Jiang W 2005 *Chin. Opt. Lett.* **3** 225
[11] Gray D C, Merigan W, Wolfing J I, Gee B P, Porter J, Dubra A, Twietmeyer T H, Ahamd K, Tumbar R, Reinholz F and Williams D R 2006 *Opt. Express* **14** 7144

[12] Kim D Y, Fingler J, Werner J S, Schwartz D M, Fraser S E and Zawadzki R J 2011 *Biomed. Opt. Express* **2** 1504
[13] Chui T Y P, VanNasdale D A and Burns S A 2012 *Biomed. Opt. Express* **3** 2537
[14] Hammer D X, Ferguson R D, Bigelow C E, Iftimia N V, Ustun T E and Burns S A 2006 *Opt. Express* **14** 3354
[15] Roorda A, Romero-Borja F, Donnelly III W J, Queener H, Hebert T J and Campbell M C W 2002 *Opt. Express* **10** 405
[16] Liu R X, Zheng X L, Li D Y, Xia M L, Hu L F, Cao Z L, Mu Q Q and Xuan L 2014 *Chin. Phys. B* **23** 094211
[17] Zhang Y, Rha J, Jonnal R and Miller D 2005 *Opt. Express* **13** 4792
[18] Liang J, Williams D R and Miller D T 1997 *J. Opt. Soc. Am. A* **14** 2884
[19] Carroll J, Neitz M, Hofer H, Neitz J and Williams D R 2004 *Proc. Natl. Acad. Sci. USA* **101** 8461
[20] Emsley H H 1953 *Visual Optics*, 5th edn. (London: Hatton Press)
[21] Grand Y L 1980 *Physiological Optics* (New York: Springer-Verlag)
[22] Hu L, Xuan L, Cao Z, Mu Q, Li D and Liu Y 2006 *Opt. Express* **14** 11911
[23] Zhang Y, Hu L, Peng Z and Xuan L 2014 *Chin. J. Liq. Crys. Disp.* **29** 709 (in Chinese)
[24] Xuan L, Li D and Liu Y 2015 *Chin. J. Liq. Crys. Disp.* **30** 1 (in Chinese)
[25] American National Standards Institute 2007 *American National Standard for the Safe Use* of Lasers (Orlando: Laser Institute of America)
[26] Lowentha S and Joyeux D 1971 *J. Opt. Soc. Am. A* **61** 847
[27] Atchison D A and Smith G 2005 *J. Opt. Soc. Am. A* **22** 29
[28] Ray S F 1994 *Photographic Lenses and Optics* (Oxford: Focal Press)
[29] McLean I S 2008 *Electronic Imaging in Astronomy: Detectors and Instrumentation* (Springer)